applied sciences

MDPI

Article

# A Novel Longitudinal Control Method Integrating Driving Style and Slope Prediction for High-Efficiency HD Vehicles

**Yifang Zhou, Mingzhang Pan, Wei Guan, Xinxin Cao, Huasheng Chen and Leyi Yuan ***

State Key Laboratory for the Protection and Utilization of Subtropical Agricultural Biological Resources, College of Mechanical Engineering, Guangxi University, Nanning 530004, China
* Correspondence: 2111391131@st.gxu.edu.cn

**Abstract:** Developing high-precision vehicle longitudinal control technology guided by ecological driving represents a highly promising yet challenging endeavor. It necessitates the fulfillment of the driver's operational intentions, precise speed control, and reduced fuel consumption. In light of this challenge, this study presents a novel vehicle longitudinal control model that integrates real-time driving style analysis and road slope prediction. First, it utilizes spectral clustering based on Bi-LSTM automatic encoders to identify driver driving styles. Next, it examines the driving environment and predicts the current slope of the vehicle. Additionally, a fuzzy controller is designed to optimize control performance, adapt to various driving styles and slopes, and achieve better fuel efficiency. The research results indicate that the DS-MPC control model developed in this paper can effectively distinguish various driving modes and has high speed control accuracy while saving 3.27% of fuel.

**Keywords:** ecological driving; slope behavior; vehicle longitudinal control; heavy-duty; model predictive control; fuel-saving

check for updates

**Citation:** Zhou, Y.; Pan, M.; Guan, W.; Cao, X.; Chen, H.; Yuan, L. A Novel Longitudinal Control Method Integrating Driving Style and Slope Prediction for High-Efficiency HD Vehicles. *Appl. Sci.* **2023**, *13*, 11968. https://doi.org/10.3390/app132111968

Academic Editor: Paolino Di Felice

Received: 8 October 2023
Revised: 19 October 2023
Accepted: 30 October 2023
Published: 2 November 2023



## 1. Introduction

The transportation system is an intricate ecosystem consisting of the interactions and limitations among people, vehicles, roads, and the environment. As the most cost-effective transportation method, road transportation involves substantial consumption of fossil fuels by heavy-duty vehicles, resulting in a growing contribution of greenhouse gases and other pollutants to global pollution sources year after year [1]. The transportation sector is responsible for generating the highest amount of greenhouse gases [2], with an estimated 30% of anthropogenic emissions attributed to it. Furthermore, the transportation sector accounts for approximately 20–25% of total energy consumption, with 65–75% of this energy being utilized for road transportation [3–5]. In recent years, many measures have been taken to optimize fuel consumption and reduce pollutants and greenhouse gas emissions in the transportation sector, including engine optimization, transmission optimization, and electric vehicle development. However, these advances are limited by technology, manufacturing conditions, and costs, making it difficult to achieve significant breakthroughs in the short term.

Vehicle technology and road environmental conditions are fundamental requirements for attaining energy-saving driving [6,7]. Speed control is a crucial component of vehicle technology development, ensuring safety while driving and reducing fuel consumption. The vehicle longitudinal control algorithm is a controller designed for speed regulation, utilizing reference and actual speeds as inputs, and throttle angle and brake position as outputs [8,9]. Several methods are available for achieving stable longitudinal control of autonomous vehicles. Simorgh [10], for instance, devised an adaptable PID controller founded on model reference, and implemented resilient update law and slope correction control in order to enhance the model's control efficiency. As technology continues to advance, numerous studies have demonstrated that modern data-based control methods can more precisely regulate vehicle speed, thereby enhancing the safety of driving. Aziziaghdam [11] devised a longitudinal controller consisting of two parts. The external controller determines the target speed, whereas the internal controller is responsible for determining the throttle and brake. Ji et al. [12] introduced a highly effective system linearization scheme that integrates a novel real-time point updating method with traditional linearization techniques. This integration leads to a reduction in steady-state errors and overshoot, ultimately improving the control performance of MPC controllers. Yang et al. proposed a new integral robust format for the asymptotic tracking of mismatched uncertain nonlinear systems [13] and a neural adaptive learning algorithm for constrained nonlinear systems with interference suppression [14], achieving the stability and accuracy of the control systems under multi-source disturbances. Li et al. [15] suggested an integrated braking and steering MPC controller that can execute accurate path tracking while retaining high computational efficiency, thereby enhancing the precision of speed control and vehicle safety.

Meanwhile, ecological driving technology [16,17], which is often overlooked, has the potential to significantly improve vehicle fuel consumption. According to research, ecological driving can decrease fuel consumption by 15% to 25% and reduce greenhouse gas emissions by at least 30% [18]. In contrast, engines and vehicles utilizing the latest technology are estimated to save approximately 10% to 12% in total fuel costs [19]. Ecological driving encompasses various factors, such as driving speed, acceleration, deceleration, route selection, and idle speed [20–22]. The variations in these factors have resulted in diverse driving styles. Deml et al. introduced a driving style classification system [23] which utilizes lateral and longitudinal acceleration behavior. Biral et al. [24] developed an objective function for risk measurement during driving, which integrates driving style and relevant safety factors into ADAS through optimal control. The concept of safe operation was integrated into the optimal control problem in the form of a penalty function. To obtain the optimal reference operation strategy, certain parameters in the driving style were utilized to optimize the control parameters.

With its robustness and easy-to-understand characteristics, fuzzy logic (FL) improves the efficiency of driving style recognition and is frequently utilized in such applications [25–27]. An FL algorithm was proposed by Syed et al. [28] to assess the ideal pedal operation of hybrid vehicles. This algorithm continuously monitors the accelerator and brake pedal operations, performs necessary corrections, and provides tactile feedback to the driver. The findings indicate that fuel consumption is cut by at least 3.5% without any impact on the vehicle's performance. Given that the initial design of fuzzy rules typically necessitates continuous experimental verification, modification, and optimization, which is both time-consuming and inefficient, machine learning methods have been widely adopted and advanced in the research of driving style recognition. By combining feature selection, machine learning models can effectively select the most representative features of the driving style from a vast array of behavioral data, resulting in a more precise identification of the driver's style. To determine the features that significantly affect fuel consumption, Jakov et al. [29] suggested a linear regression model that takes into account ten features that directly reflect fuel consumption, aiming to identify variations in driving behavior. Tao et al. [30] investigated the features of driving cycles by employing genetic algorithms, wherein they selected six out of twelve features under sampling windows of 146 s and 80 s. Yang et al. [31] employed a Gaussian mixture model to determine the feature distribution that influences driving style and employed Bayesian information to evaluate and analyze the correlation of the selected features.

It is necessary to take into account the road slope for eco-friendly driving while on the road. When compared to the traditional adaptive cruise control (ACC) system, the ecological driving technology that incorporates road slope information in advance has been found to enhance fuel economy by 4.5%. Consequently, the integration of road slope factors into the longitudinal control methods of automobiles has garnered significant research interest. Sun et al. [32] introduced a hybrid model predictive control (HMPC) theory and employed a mixed logic dynamic (MLD) framework, a specialized hybrid system modeling technique, for the development of the upper controller. The proposed control method's effectiveness was verified through the use of speed tracking at various slopes and NEDC loops for speed tracking. Andreas et al. [33] proposed an energy-optimal adaptive cruise control method that takes into account factors such as speed limits, road slope, and travel time during the optimization process, resulting in the planning of an optimal speed trajectory. Zhai et al. [34] proposed a distributed model predictive control method for vehicles driving on highways with various slopes. When compared to benchmark testing, the proposed strategy can result in saving more than 21% of fuel for the entire vehicle.

This article aims to improve the speed control accuracy of heavy-duty truck driving assistance systems and simultaneously reduce fuel consumption by constructing a high-precision vehicle longitudinal control model guided by ecological driving. The structure of this article is as follows. In Section 2, the process of establishing an MPC speed control model that integrates driving style recognition methods and road slope is discussed in detail. In Section 3, the data sources are examined and the efficacy of the model is confirmed. Subsequently, the model built in this article was simulated and validated by setting different road slope conditions. Simultaneously, in Section 4, an accurate analysis is conducted on the effectiveness of the DS-MPC control method under real driving conditions. Finally, the main findings are summarized and future work is discussed in Section 5.

## 2. The Design of the Control System

### 2.1. Calculation of the Slope

In this paper, the slope of the actual road is calculated based on the vehicle speed and GPS elevation information collected by the CAN bus, and the calculation is shown in Equation (1).

At low slope angles,

$$tan\left(\frac{H}{L}\right) \approx sin\left(\frac{H}{S}\right) \tag{1}$$

where, $H$ is the GPS elevation, $S$ is the actual distance travelled by the vehicle, and $L$ is the straight-line distance between GPS elevations. Then the slope $i$ can be expressed as Equation (2).

$$i = \arcsin\left(\frac{H}{S}\right) = \frac{H_2 - H_1}{(V_2 + V_1) \times \Delta t} \times 2 \times 3.6 \tag{2}$$

where $\Delta t$ is the time taken to travel from $H_1$ to $H_2$. $v_1$ and $v_2$ are the speed at $H_1$ and $H_2$, respectively.

As can be seen from Equation (2), GPS elevation and vehicle speed are important indicators for determining slope and in the actual data collection process, there may be cases of missing or abnormal data. In the case of missing or abnormal elevation data, the process shown in Figure 1 is used for elevation correction. For vehicle speed, when the vehicle is in the parking state ($v = 0$), its GPS elevation should remain unchanged, so its slope remains unchanged, and the slope of the current position is filled with a similar reasonable value. In the abnormal state of vehicle speed data, linear interpolation is used for the correction.

### 2.2. Feature Selection

A feature selection method based on a sigmoid function-based whale optimization algorithm is used according to the requirement for the feature selection of natural driving data. The features most relevant to driving style expression are selected by limiting the range of output values in the location update phase in order to reduce the size of the dataset used for driving style recognition while retaining relevant information. In this paper, the k-means method is used to construct the initial features for driving style feature recognition.

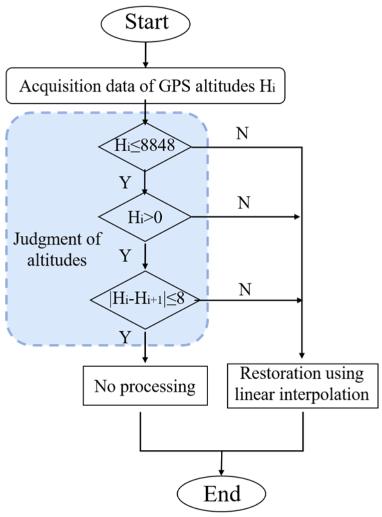


**Figure 1.** GPS altitude correction process.

To complete the feature selection associated with driving style, the continuous WOA must be converted to its corresponding binary space [0, 1]. The use of a sigmoid transfer function can force the search agent to move through the binary space [35,36], thus improving the whale optimization algorithm for driving style feature selection. The equation is defined as shown in Equation (3).

$$S(\Delta X_t) = \frac{1}{1 + e^{-\Delta X_t}} \tag{3}$$

where, $\Delta X_t$ denotes the step vector of the search space at. Thereafter the current search agent uses Equation (4) to complete the position update.

$$X_{t+1}^{d}(t+1) = \begin{cases} 1 & if \quad rand < S(\Delta X_{t+1}) \\ 0 & if \quad rand \geq S(\Delta X_{t+1}) \end{cases} \tag{4}$$

where, $rand$ denotes a random number in (0, 1).

The objective of feature selection is to find the minimum number of features to select and to obtain the maximum classification accuracy. Based on this objective, both objectives are aggregated and transformed into a single objective problem as in Equation (5), and the minimum fitness value is defined as the sum of the small classification error rate and the minimum number of selected features.

$$Fitness = \lambda \times E_r + \eta \frac{|S_l|}{|F_l|} \tag{5}$$

where, $E_r$ denotes the classification error rate and $S_l$ , $F_l$ are the length of the selected feature subset and the number of all features, respectively. $\lambda$, $\eta$ are the degree of importance of classification accuracy and feature subset length, and $\lambda + \eta = 1$. In this paper, we take $\lambda = 0.99$. The fitness value of each solution is continuously calculated during the iterative process and the subset with the smallest fitness value is treated as the optimal solution, based on which the classification accuracy is calculated as in Equation (6).

$$Accuracy = 1 - E_r \tag{6}$$

To avoid over-fitting in subsequent calculations, highly correlated features need to be removed. In this paper, the Pearson correlation, a measure of linear correlation between two variables, is used to identify and remove highly correlated features from the dataset, allowing the model to focus on the most informative features, thereby improving generalization and performance. It is calculated as in Equation (7).

$$\rho_{X,Y} = corr(X,Y) = \frac{cov(X,Y)}{\sigma_X \sigma_Y} = \frac{\sum_{i=1}^{n}(X_i - \bar{X})(Y_i - \bar{Y})}{\sqrt{\sum_{i=1}^{n}(X_i - \bar{X})^2}\sqrt{\sum_{i=1}^{n}(Y_i - \bar{Y})^2}} \tag{7}$$

where, $cov(X,Y)$ are the covariances of the variables $X$ and $Y$. $\sigma_X$, $\sigma_Y$ are the standard deviations of the variables $X$ and $Y$. $\bar{X}, \bar{Y}$ are the arithmetic mean of the samples $X_i$ and $Y_i$. The value ranges from $[-1, 1]$, where the closer it is to 1 or $-1$, the stronger the linear relationship between the features, and the closer it is to 0, the weaker or no relationship between the features.

### *2.3. Driving Style Recognition*

The spectral clustering algorithm, derived from graph theory [37], is a method that utilizes the spectral properties of data to simultaneously perform dimensionality reduction and clustering. The basic idea behind spectral clustering is to convert the data into a graph representation and use the eigenvectors of the graph Laplacian to project the data into a low-dimensional space where clustering can be performed more efficiently. Spectral clustering is flexible and can handle complex and nonlinear data structures, so it is commonly used with driving style recognition. Spectral clustering is highly scalable, can handle large datasets, is computationally efficient, and is well suited to handle large amounts of driving data. In addition, spectral clustering is robust to noise and outliers, which makes it accurate in recognizing driving styles even when natural driving data is noisy.

The combination of Bi-LSTM and a self-encoder is shown in Figure 2. The self-encoder compresses the data to low dimensions and later uses the compressed data as input, and the trained Bi-LSTM network learns the temporal dependencies between the sequence data points. In the training phase, the auto-encoder and Bi-LSTM networks are jointly trained, and this joint training process helps the model to learn a more informative and compact representation of the input data, which improves the performance of the driving style recognition task.

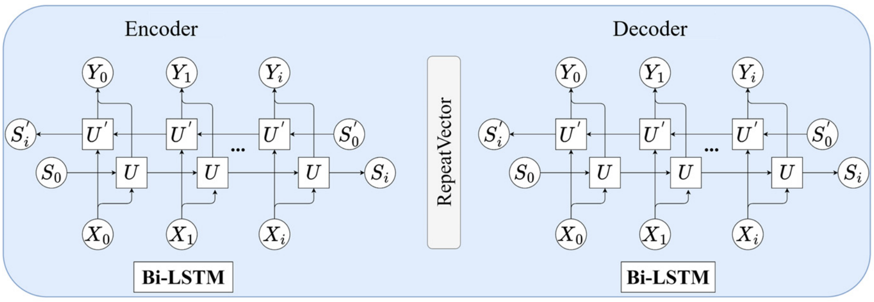


**Figure 2.** Schematic diagram of Bi-LSTM combined with autoencoder.

Currently, the use of machine learning for driving style recognition is inefficient, costly, and weak in practical applications under large data conditions. Natural driving data is a continuous time series, and the state of the data at the current moment is related to the state of the moments before and after. Therefore, a spectral clustering driving style recognition method based on a Bi-LSTM autoencoder is proposed, which firstly determines the original labels from the cleaned data using k-means, and then uses a whale optimization algorithm combined with a sigmoid function to compress the size of the data set and use it for The selected features are fed into an auto-encoder with Bi-LSTM to learn the feature values and feature vectors required for spectral embedding, and spectral clustering is used to determine the driving style, as shown in Figures 3 and 4. The red and green lines in Figure 4 represent the flow of data at different layers.

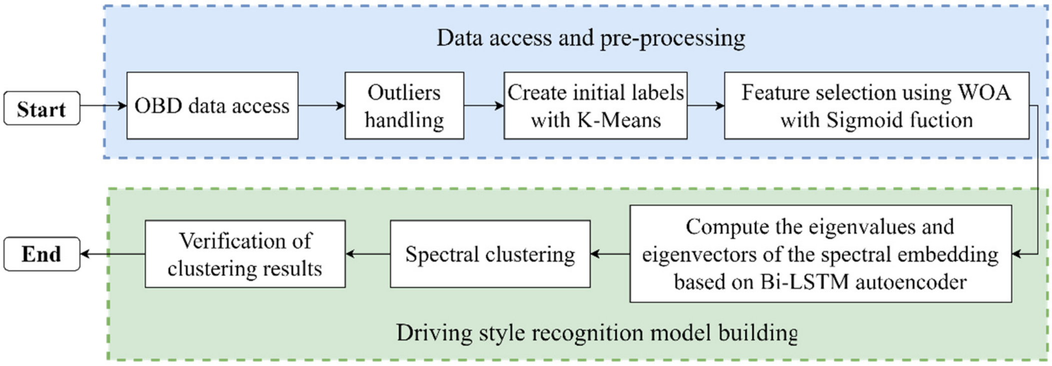


**Figure 3.** Framework of driving style recognition.

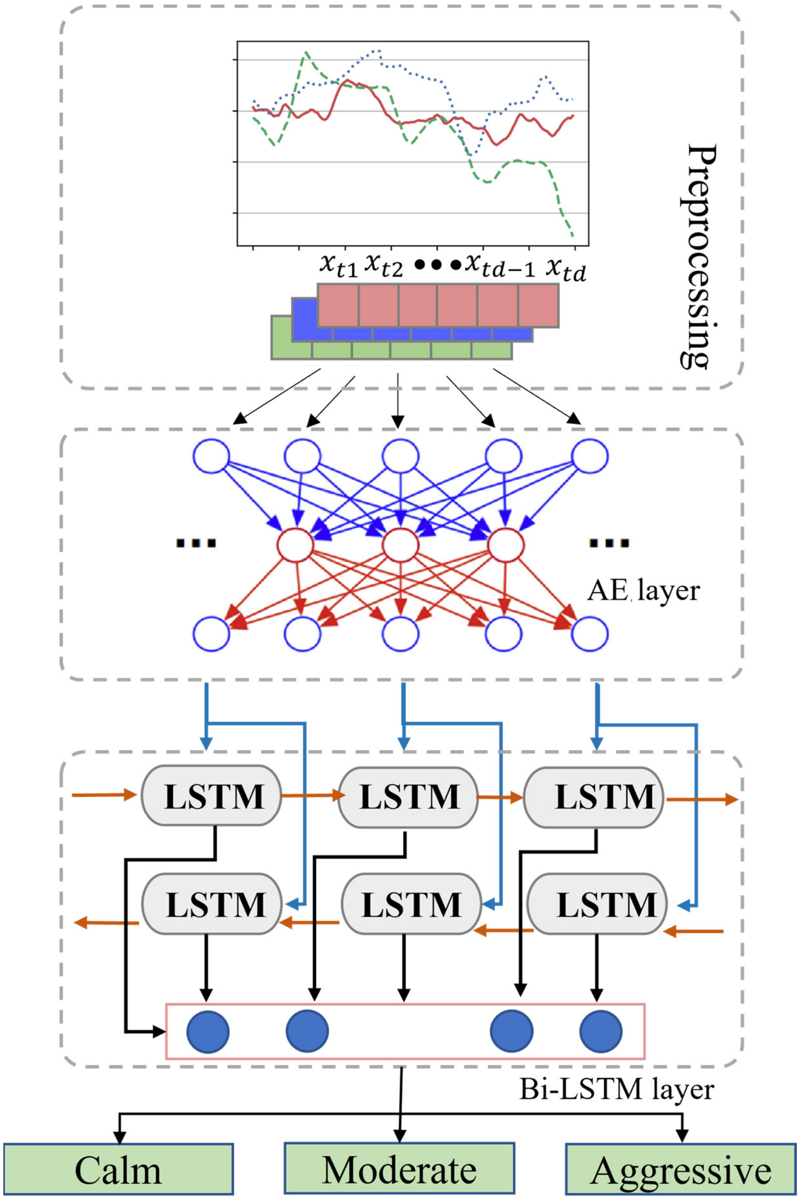


**Figure 4.** Model of driving style recognition.

In order to enable real-time feedback control of the vehicle based on the driver's driving style and road slope, this chapter proposes a model predictive control method with adaptive weights for the longitudinal control of the vehicle based on the driver's driving style and changes in road slope, thus achieving real-time feedback on changes in driving operation requirements based on optimization control.

### *2.4. Fuzzy Logic*

Traditional control methods require the establishment of a mathematical model of the control system, but for some control objects with complex structures and unknown mechanisms, traditional control methods cannot be controlled. Fuzzy control is a control technique that uses fuzzy logic to deal with uncertainties and inaccuracies in control systems. Fuzzy logic reasoning is a method based on empirical summaries whose rules can be expressed in natural language without the need to know the mathematical model of the control object. Therefore, fuzzy logic reasoning is particularly suitable for control objects where it is difficult to obtain mathematical models and dynamic characteristics and has the advantages of robustness and adaptability. In MPC, the use of fuzzy logic reasoning can improve the accuracy of the models used for prediction and control. A driver's driving style can be thought of as a set of preferences and rules that govern the way the driver operates the vehicle. Incorporating these preferences and rules into the control system through fuzzy control allows the control system to adapt to the driver's style, improving driving comfort and safety.

The basic idea of fuzzy logic reasoning in MPC is to improve the accuracy of the predictive model by adjusting the subordination function used in fuzzy logic to deal with the relationship between the various variables in the control system, and thus predict and control the actions more accurately. Traditional predictive control models with fixed parameters do not respond quickly enough to the driver's actions, which can affect the smoothness of the driving operation. In addition, road slope conditions affect driver performance and fuzzy logic reasoning can improve the adaptability of the model predictive control model to the environment. Therefore, this paper uses a fuzzy control approach to adaptively adjust the weighting factors with changing operating conditions and uses the Fuzzy Logic Designer tool in MATLAB to complete the construction of the model.

#### 2.4.1. Fuzzy Logic Reasoning Framework Design

In MPC, the model parameters mainly include the prediction time domain $N_p$, the control time domain $N_c$, the error weight matrix $Q$, and the control weight matrix $R$ in the objective function equation. The selection of the parameters directly affects the effectiveness of the MPC. To this end, weights that reflect the system's ability to follow the reference trajectory are controlled in the objective function to be optimized to reflect the influence of driving style and road environment. The driving style and road slope have a certain stability in the secular data, and to assist in reflecting the influence of driver behavior and road environment, the actual vehicle speed and acceleration rate of change are added as errors along with the input to the fuzzy logic. Therefore, a four-dimensional fuzzy controller was designed based on driving style, current road slope, current vehicle speed, and acceleration rate of change, as shown in Figure 5.

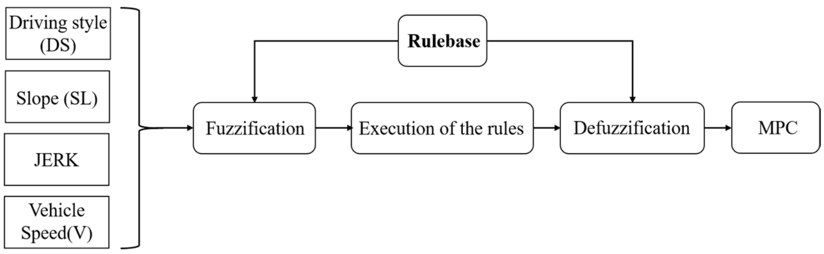


**Figure 5.** Schematic diagram of fuzzy logic reasoning.

The driving style is based on the above recognition results, the slope can be calculated in real time based on the vehicle speed and GPS information, while the acceleration rate of change and the vehicle speed can be obtained based on the vehicle's motion state, and then the error weighting factor $Q\prime$ can be obtained after fuzzy inference, and the corresponding weighting factor $Q$ can be obtained after defuzzification. Therefore, the adjustment of the error weight factor is carried out adaptively in real time and the results are fed into the model predictive control model in real time.

### 2.4.2. Fuzzification

Fuzzification is the process of converting explicit inputs into fuzzy variables or fuzzy sets. In fuzzy control, the aim of fuzzification is to map explicit inputs into linguistic variables that can be used for fuzzy rule bases and inference.

Combined with the input fuzzy control in this paper, $DS$ represents driving style whose discrete domain is [−1, 0, 1], $SL$ represents slope whose continuous domain is [−8, 8], $Jerk$ represents rate of change in acceleration whose continuous domain is [0, 10], $Vel$ represents vehicle speed whose continuous domain is [0, 100] and the continuous domain of the output variable is [10, 20].

Based on the changes in the input and output variables, the corresponding fuzzy linguistic variables are defined so that the corresponding knowledge base can be constructed, as in Equation (8).

$$\begin{gathered} DS = \{NB, Z, PB\} \\ SL = \{NB, NS, Z, PS, PB\} \\ Jerk = \{NB, Z, PB\} \\ Vel = \{NB, Z, PB\} \\ Q = \{NB, NS, Z, PS, PB\} \end{gathered} \tag{8}$$

where, $NB$ is negative big, $NS$ is negative small, $Z$ is positive medium, $PS$ is positive small, and $PB$ is positive big.

The affiliation function selected for driving style is a triangular distribution, while the remaining input and output variables use a combination of triangular and trapezoidal distributions. The affiliation function for each input and the affiliation function for the output are shown in Figure 6.

### 2.4.3. Fuzzy Rule Design

The rate of change in acceleration is most pronounced when the driver has an aggressive driving style and is more similar for different slope conditions. The driver's output increases from 0 (Z) to positive (PB) in the acceleration rate of change domain when driving uphill or downhill, depending on their speed change, where a more conservative output is favorable if the slope is gentle. The effect of speed variation is more pronounced when the driver is a normal type of driving style. Drivers in this category usually have limited acceleration variation, i.e., they do not accelerate or decelerate as often, and are considered to be operating more steadily up and down hills, so their output is maximized only at high slopes, high speeds, and high rates of changes in acceleration. When the driver has a conservative driving style, in order to show the difference from a normal driver, it is assumed that he or she will adopt the most conservative operating strategy in the uphill and downhill conditions and will usually adopt a low speed and low change in acceleration strategy to pass, so the output usually varies from negative big (NB) to positive small (PS). Similar to the moderate driver, the maximum is only reached at high slope, high speeds, and high rates of changes in acceleration. Based on the above design of the fuzzy rules, a total of 135 fuzzy rules were designed and Figure 7 shows the design surface corresponding to the fuzzy rules.

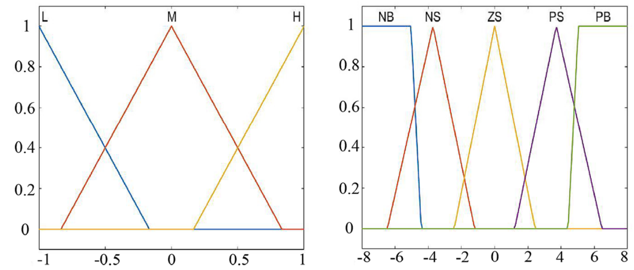


(a) The affiliation function of driving style

(b) The affiliation function of slope

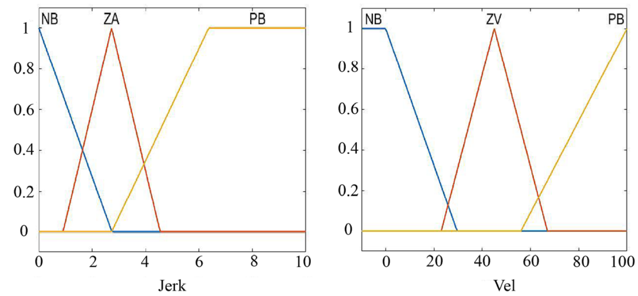


(c) The affiliation function of jerk

(d) The affiliation function of vehicle speed

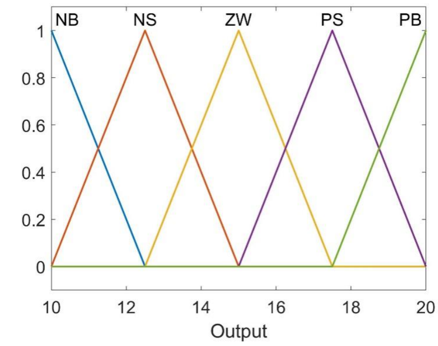


(**e**) Fuzzy logic output affiliation function

**Figure 6.** Plot of affiliation functions for fuzzy logic input and output.

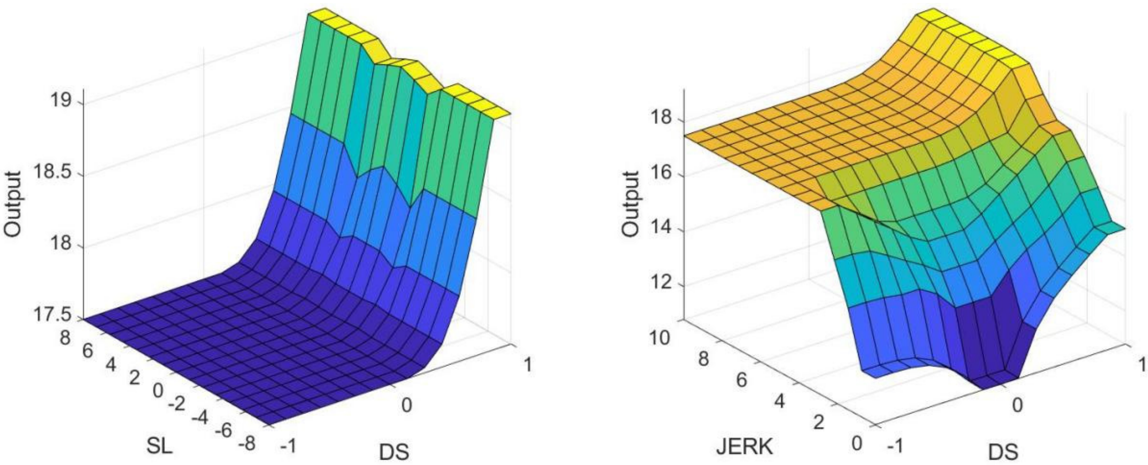


**Figure 7.** *Cont*.

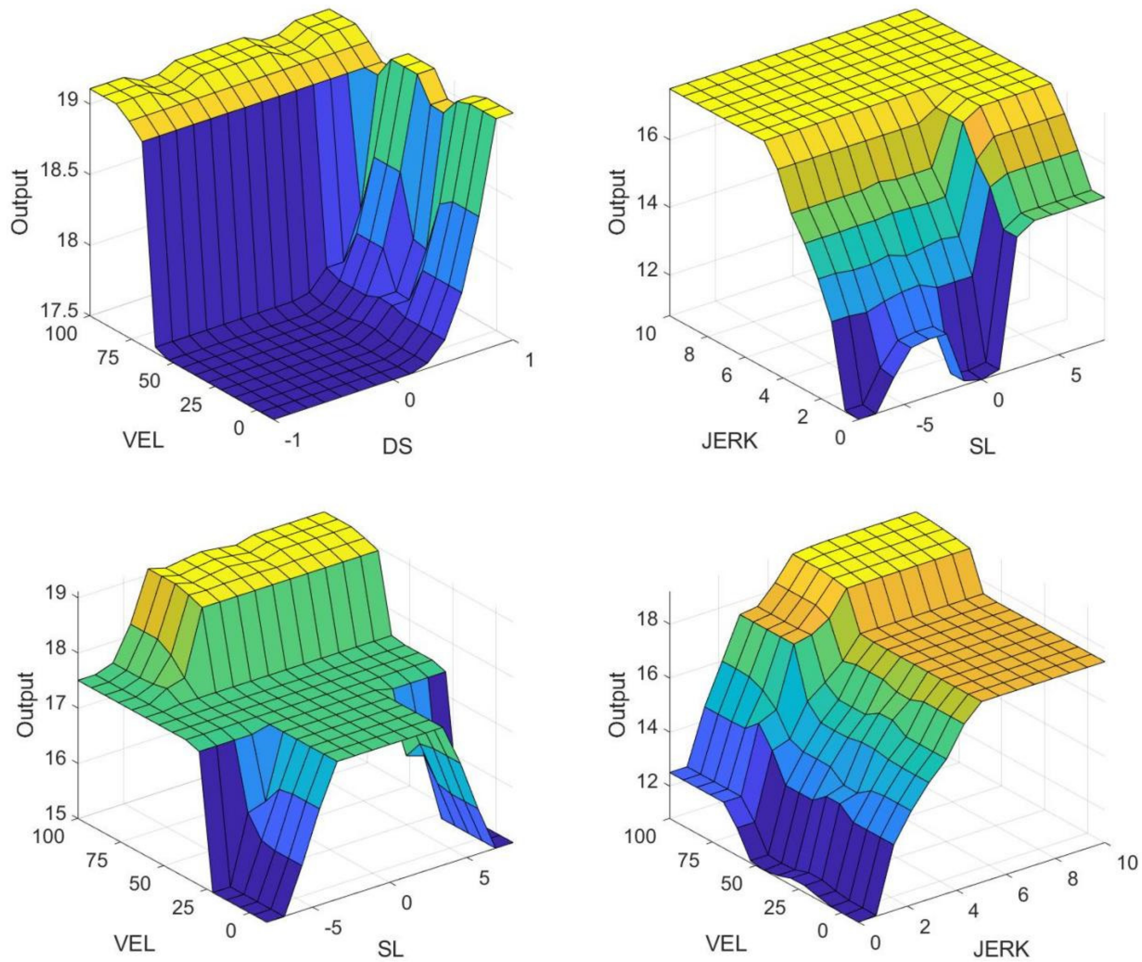


**Figure 7.** Design surface diagrams of fuzzy rules.

According to different driving styles, slope changes, speed, and rates of changes in acceleration, the value of the error weight $Q$ is adjusted in real time and the optimization problem can be solved through quadratic planning, so that the design of the model prediction control model based on driving style is completed.

### *2.5. Model Predictive Control Considering Driving Style and Slope*

Model predictive control is a feedback control algorithm that solves a multi-objective optimization problem in the predictive time domain in real time online based on a dynamic mathematical model of the system, and then calculates the most appropriate control action and achieves control of the system through continuous iterative operations. The algorithm has the advantages of generalization, immunity to disturbances, robustness, and excellent dynamic performance, without the need for an exact model. Therefore, model predictive control can be a good solution to the problems of model mismatch, time lag, and non-linearity caused by the complex environment of the vehicle.

The basic principle of model predictive control is to predict the future output of the system based on the existing model, the current state of the system, and the future control quantities, and to achieve the control purpose by solving the constrained optimization problem on a rolling basis, with three basic properties: predictive model, feedback correction, and rolling optimization.

Due to the time lag in the braking system, the engine system, and the acquisition and processing of sensor signals, there is a delay between the actual acceleration and the desired acceleration during the longitudinal motion of the car. In order to track the desired acceleration more accurately, the tracking of the car's acceleration can be considered as a first-order inertial link and incorporated into the control system, whose transfer characteristics can be expressed as Equation (9).

$$G(s) = \frac{K}{\tau \cdot s + 1} \tag{9}$$

where, $K$ is the link gain. In model predictive control based on driving style, the influence of driving style constraints on the state and control quantities of the system needs to be considered. In this study, the driving style constraints are mainly manifested as the effects of acceleration and acceleration rate of change, with different constraints for the acceleration and deceleration conditions, respectively.

For an aggressive driving style, drivers will use greater throttle opening, faster acceleration, and a higher rate of change in acceleration when accelerating, higher deceleration, and a wider opening of the brake pedal when decelerating, while normal and calm drivers will be more cautious, so the constraints on acceleration and the rate of change in acceleration are shown in Equations (10)–(12).

$$u_{min} \le u(k+i) \le u_{max}, i = 0, \ldots, \ N_c - 1 \tag{10}$$

$$\alpha \Delta u_{min,ac} \le \Delta u_{ac}(k+i) \le \alpha \Delta u_{max,ac}, i = 0, \ldots, N_c - 1 \tag{11}$$

$$\alpha \Delta u_{min,de} \le \Delta u_{de}(k+i) \le \alpha \Delta u_{max,de}, i = 0, \ldots, N_c - 1 \tag{12}$$

In the above equations, $U$ is the acceleration constraint and the lower two rows are the acceleration change constraint on acceleration and the acceleration constraint on deceleration, respectively. For the effect of driving style, $\alpha$ = 1.2 for aggressive drivers, $\alpha$ = 1 for moderate drivers and $\alpha$ = 0.8 for calm drivers, as below. Equations (13) and (14) were used to make decisions about their rate of change in acceleration.

$$\Delta u_{min} \le \Delta u(k+i) \le \Delta u_{max}, i = 0, \ldots, \ \ N_c - 1 \tag{13}$$

$$\Delta u_{max} = \begin{cases} \alpha \Delta u_{max,ac} & \text{if } a_{des}(k-1) \ge 0 \\ min(\alpha \Delta u_{max,de}, \alpha \Delta u_{max,ac} - a_{des}(k-1)) & \text{if } a_{des}(k-1) < 0 \end{cases} \tag{14}$$

In this section, according to the aforementioned adaptive model predictive control with driving style recognition and fuzzy rule construction, an adaptive model predictive control model considering driving style and slope was constructed using Carsim 2019.1 and MATLAB/Simulink 2018a. The model built in this paper was validated by setting different road conditions of slope and real driving conditions.

An adaptive model predictive control model considering driving style as shown in Figure 8 was constructed by means of Carsim, MATLAB/Simulink.

The joint simulation platform is divided into four main parts, including the upper model predictive control part, the lower speed controller part, the vehicle model part, and the fuzzy inference part. The upper controller, lower speed controller and fuzzy inference sections were implemented in the main runtime environment of MATLAB/Simulink, and the vehicle model section was built in the Carsim 2019.1 simulation software. The vehicle model is used to transmit the vehicle configuration and parameter states to the upper model predictive control and fuzzy inference logic in real time during simulation time. The upper controller transmits the desired acceleration decision to the lower control strategy based on the results of the fuzzy inference, the desired speed sequence, and the actual vehicle longitudinal speed. The lower-level speed controller obtains the corresponding brake cylinder pressure or throttle opening according to the desired acceleration and inputs it to the vehicle model, which determines the braking or driving state of the vehicle according to the input signal, forming closed loop control.

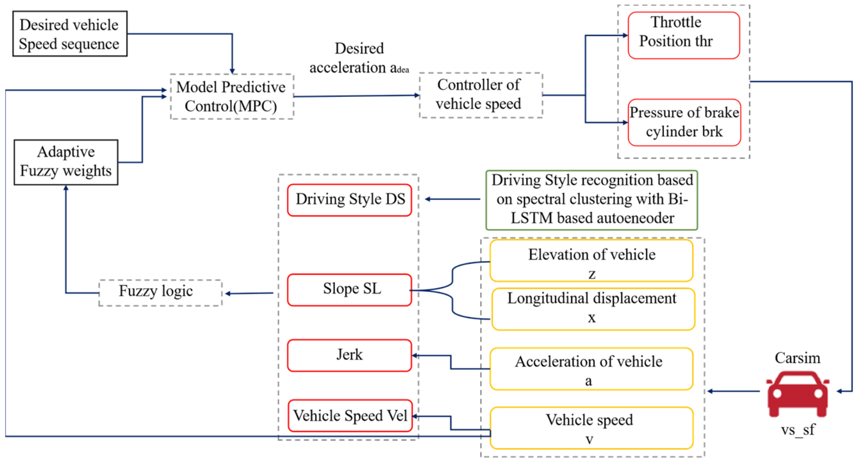


**Figure 8.** Diagram of the adaptive model prediction control simulation platform considering driving style and slope.

This section takes the fuzzy inference module and uses driving style, slope, rate of change in acceleration, and speed as inputs to the fuzzy controller and thus obtains the control quantity weights $Q$ for the model predictive control, which in turn expresses the effect of driving style on vehicle control. In this condition, the vehicle is simulated for uphill and downhill conditions at 0% and 5% slopes.

## 3. Simulation and Verification

### *3.1. Verification of the Driving Style Recognition Model*

In this paper, five semi-trailers were used for the study. To reduce the influence of vehicle performance and driving sections on driving operation, the batch of vehicles had the same engine parameters and were driven on the same test section of the Guangkun Expressway G80. All vehicles were driven by experienced drivers and the drivers were not informed in any way during the experiment to avoid the influence of the driver's psychological state on the experiment. On board diagnostics (OBD) was installed on the experimental vehicles from which the relevant data fields were extracted at the end of the journey on the experimental section and the data was uploaded via the CAN bus to complete the acquisition.

Considering the instability of the sensors, some of the raw data were lost or abnormal, so the box plot method was used for data cleaning and interpolation was used to fill in the data. In addition, considering that continuous prolonged parking is not beneficial for driving style segmentation, it was removed together with the data cleaning process.

A box-and-whisker plot [38] is a graphical representation of a dataset that displays, in a compact and standardized manner, information about the location, dispersion, degree of dispersion, and crosstabulation of anomalous observations. Typically, a box plot as shown in Figure 9 consists of four parts: the median, the box, the tentacles extending from the box, and the outliers. The process of processing anomalous data using the box plot method is shown in Figure 10. Considering the continuity of the second data and their changing characteristics during the data acquisition process, it is highly reliable to use the linear interpolation method for data correction based on the elimination of outliers.

Taking the vehicle driven by driver number 47 as an example, this paper uses the k-means method to initialize the markers of the original data. The definition of driving style varies from scholar to scholar and is usually classified into 2–4 categories. Considering the practical significance of driving style, the clustering results are divided into three categories in this paper.

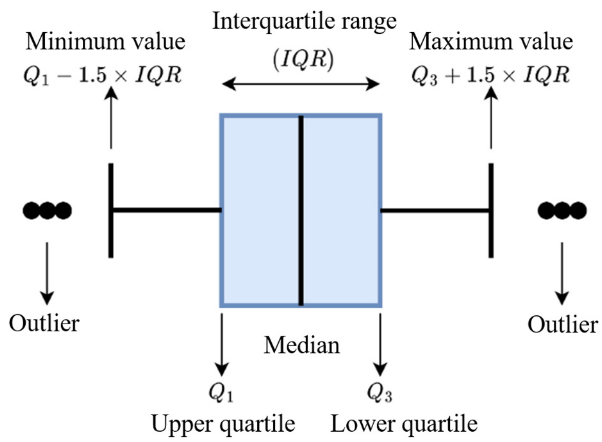


**Figure 9.** Schematic diagram of the box plot method.

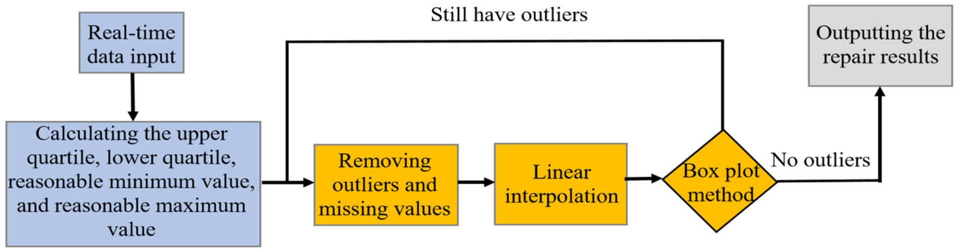


**Figure 10.** Abnormal data processing process.

The data with initial labels obtained from K-means were imported into the whale optimization algorithm for feature selection, and after several tests and parameter adjustments, the number of search agents and the number of iterations were set to 16 and 70, respectively. 97.34% of the features were selected accurately according to the fitness function used in this paper. In order to verify the relevance of the selected features, Pearson's correlation coefficient method was used to determine the relevance of the features, and it was found that the correlation coefficient between throttle opening and cyclic fuel injection amount reached 0.97. Taking into account the correlation between the features, the feature of throttle opening was excluded. The correlation results for the remaining features are shown in Figure 7, indicating that the selected features are relatively independent and can be used to analyze the influence on driving style.

To avoid overfitting problems caused by too many layers in the self-encoder, two Bi-LSTM layers with 32 cells are used as an encoder and decoder in the self-encoder. The selected features were also applied to the self-encoder as input. Based on several tests of the model, the models with 80 epochs and 32 batches were trained using TensorFlow, respectively, to improve the training efficiency of the model while maintaining accuracy. Finally, the weight matrix obtained through training is applied to the eigenvalues and eigenvectors of the spectral embedding to calculate the driving style recognition results.

Table 1 shows the rates of change in the above variables, and it can be seen that the rates of change in torque, intake pressure, and recirculating fuel injection have some similarity within the corresponding driving style intervals, and the corresponding aggressive, moderate, and calm driving characteristics are defined according to the magnitude of their values. According to the feature selection, even though torque and intake pressure are not included in the selected features, the feature selection and driving style identification results reflect the variation pattern of both.

**Table 1.** The average rate of change for each driving style corresponding to the selected characteristics.

| | Torque | Inlet Pressure | Injected Fuel Quantity | Throttle Position |
|---|---|---|---|---|
| Aggressive | 301.92 | 111.84 | 29.15 | 10.86 |
| Moderate | 186.30 | 72.38 | 19.31 | 5.89 |
| calm | 44.12 | 61.39 | 3.98 | 1.42 |

Three typical segments of the vehicle belonging to driver number 47 were selected with 140 consecutive sampling points to explore the differences between the driving styles. Considering the transfer characteristics of the data in the self-encoder-based Bi-LSTM, the driving style segmentation could not be continuously consistent, so the three selected typical segments were divided into aggressive, moderate, and calm driving styles, as shown in Figure 11.

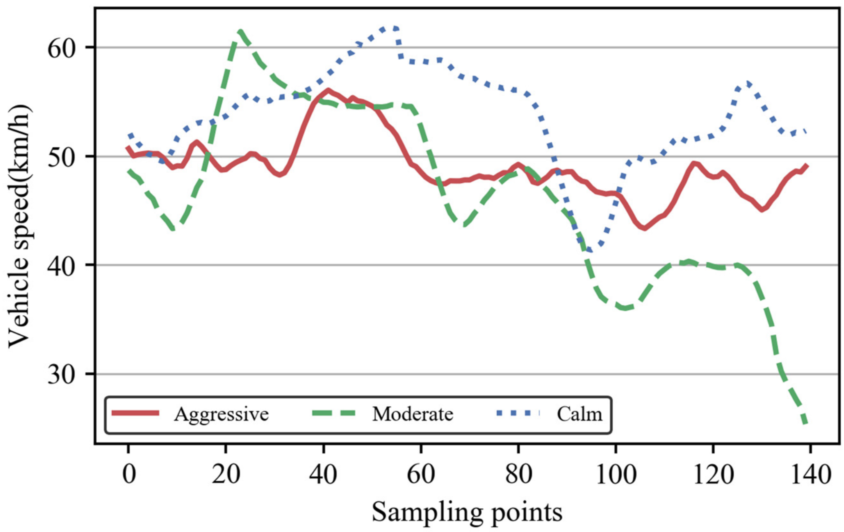


(**a**) Continuous sampling chart of vehicle

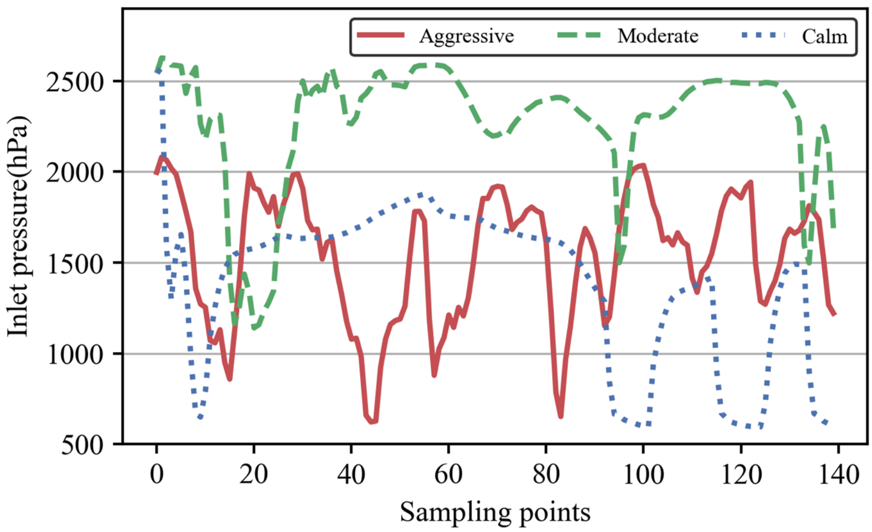


(**b**) Continuous sampling chart of inlet

**Figure 11.** *Cont.*

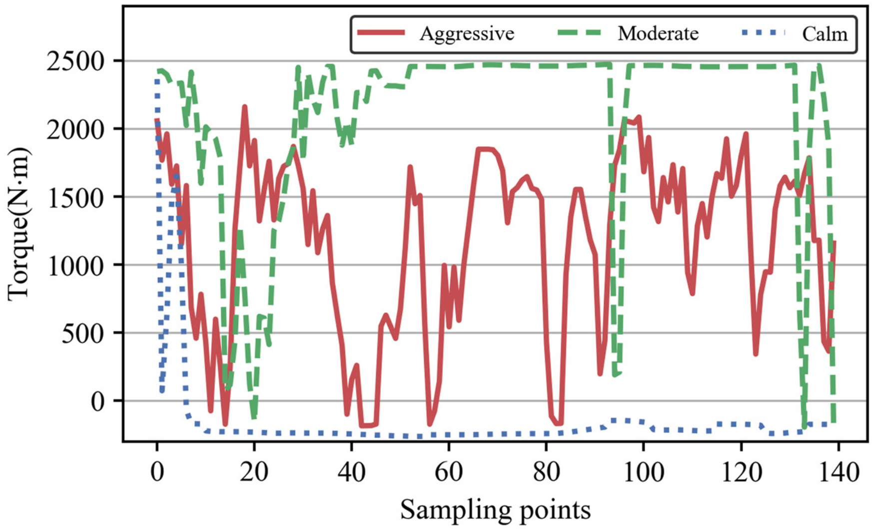


(**c**) Continuous sampling chart of torque

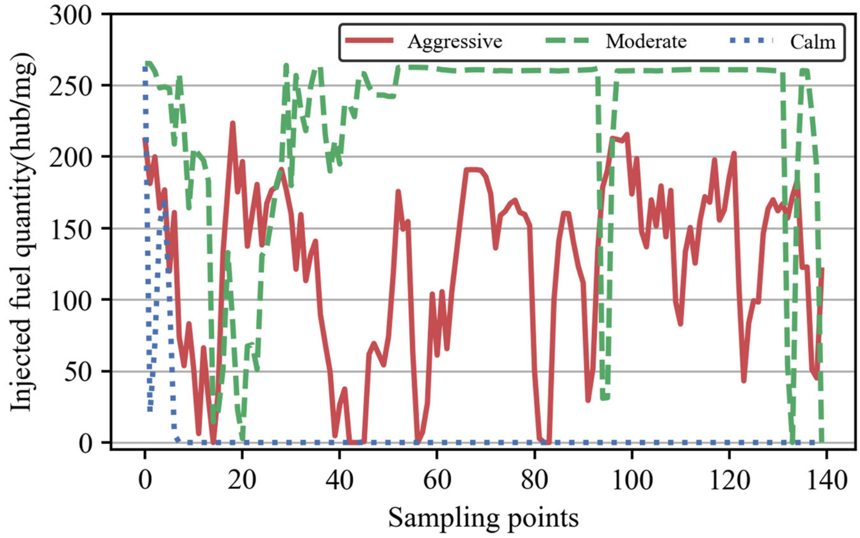


(**d**) Continuous sampling chart of injected

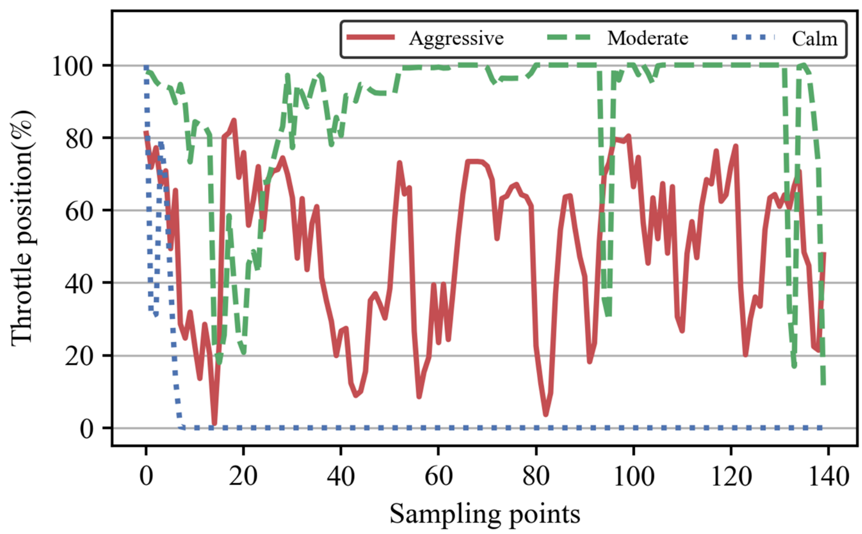


(**e**) Continuous sampling chart of throttle

**Figure 11.** Sampling points of vehicle No. 47.

Overall, as the driver changed gear and throttle operation, the vehicle's corresponding speed, torque, intake pressure, and cyclic fuel injection produced corresponding rapid changes. Combined with Table 1, even though the values of the indicators were larger for the moderate driving style, the rate of change is low, indicating that the driver maintained a relatively stable driving condition during the driving process. In the case of the calm driving style, the driver did not operate the throttle or gears, but the vehicle still kept moving forward, so it could be assumed that the vehicle was going downhill and there were no obvious sudden changes in the vehicle's state. The driving style recognition model proposed in this paper is effective.

### 3.2. Effectiveness Analysis of DS-MPC Method under 5% Slope

Under this operating condition, the vehicle was driven on flat ground at 0–5 s, uphill at 5% after 5 s, with no slope at 25–35 s, downhill at 5% at 35–55 s, and ended on flat ground at 55–60 s. Figure 12 shows the tracking of the vehicle speed under this operating condition. Overall, the vehicle speed was slightly below the reference value when driving in the calm driving style, while the moderate and aggressive styles were slightly above the reference value, in line with the previous description of driving styles. At the same time, the aggressive and moderate styles were more responsive than the calm style when reaching maximum speed, and they shifted earlier when shifting downhill. On a steeper slope, the aggressive driving style control response was faster, but it also increased the instability of the system.

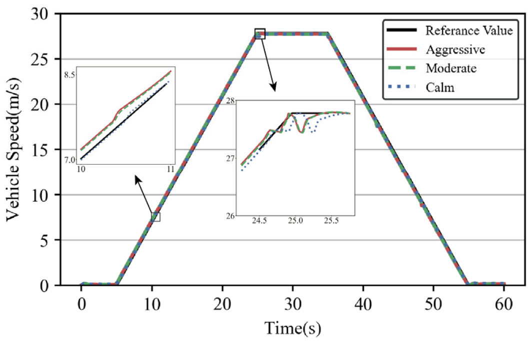


**Figure 12.** Speed tracking curve for drivers with different driving styles.

Figure 13 reflects the fuel consumption at a 5% slope. Overall, more fuel was consumed accelerating uphill than decelerating downhill, which is in line with reality. In the uphill phase, the aggressive driving style consumed more fuel more quickly as it needed to maintain a higher speed variation, whereas the calm driving style consumed less fuel as the speed on the uphill was closer to the desired speed and the speed variation was smoother.

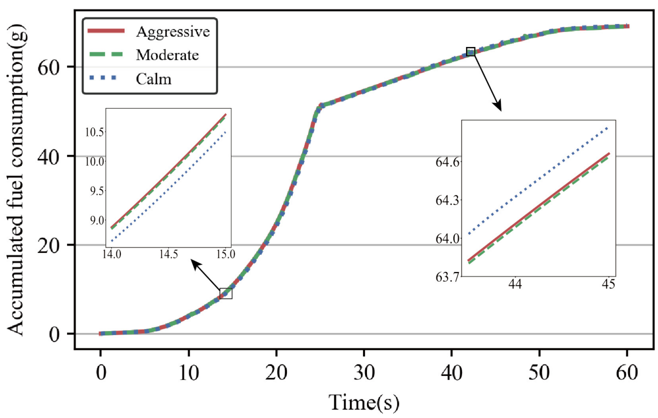


**Figure 13.** Fuel consumption change curve of drivers with different driving styles.

The brake cylinder pressure change curve for drivers with different driving styles is shown in Figure 14. In the downhill phase, the calm driving style produced higher fuel consumption due to frequent driver braking, resulting in frequent speed changes, while the aggressive and moderate driving styles consumed similar fuel and were comparable to their descriptions.

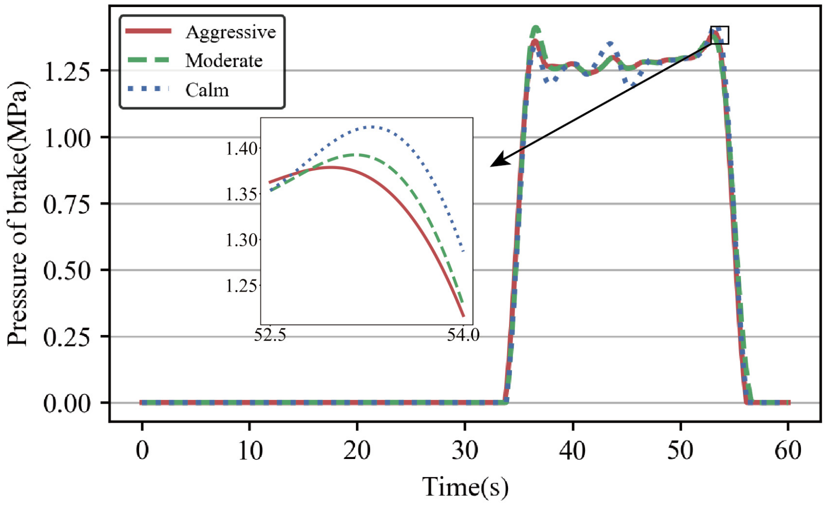


**Figure 14.** Brake cylinder pressure change curve for drivers with different driving styles.

### *3.3. Effectiveness Comparison of the DS-MPC Method under 0% and 5% Slopes*

Considering both driving style and slope in the predictive control of the model can further reflect the interaction between the driver and the driving environment. In different driving environments, drivers will adjust their driving behavior in real time according to the changing environment and the influence of driving style will make some difference. Figure 15 shows the speed tracking of different driving styles on different slopes. It can be seen that during acceleration, acceleration was faster on flat ground (0% slope) and slower on longitudinal slopes. Similarly, during deceleration, the deceleration was smoother on flat ground. When a smooth speed was reached, the change in speed was smoother on the flat ground than on a 5% slope, with no jumps occurring. The distribution of driving styles is more similar on the flat ground, while on a 5% slope there is a clearer distinction, indicating that the influence of the driving environment on the driver's handling of the vehicle should not be ignored.

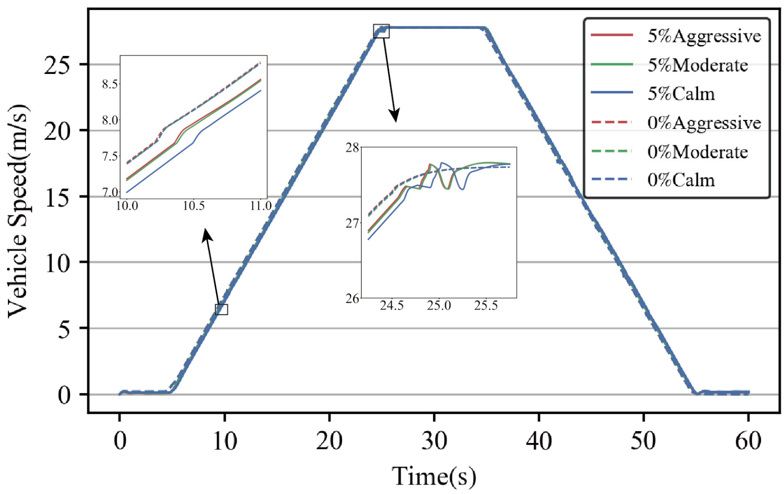


**Figure 15.** Variation of speed tracking for drivers with different slopes and different driving styles.

Figures 16 and 17 show the variation curves of throttle opening and brake cylinder pressure corresponding to different slope and different driving styles. Combined with the graphs, it can be seen that the same speed control strategy can be achieved with a smaller throttle opening on flat ground, with less variation between driving styles. Similarly, for braking, the behavior of the different driving styles on flat ground tends to be similar and smoother with a 5% slope, and there was no jump in the braking process. In the case of a single driving environment, the influence of driving style on driving behavior is weaker, and the main influence comes from the change in speed.

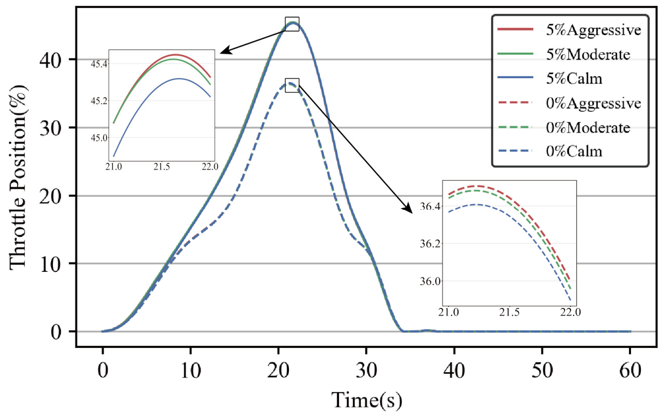


**Figure 16.** Different slope, different driving style vehicle throttle opening change curve.

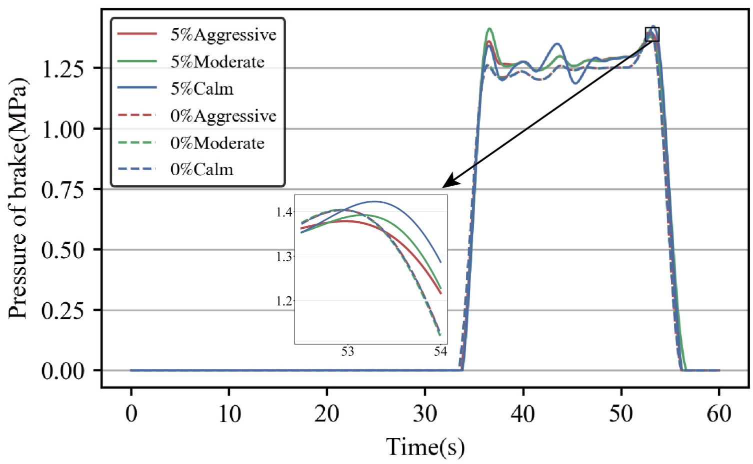


**Figure 17.** Different slope, different driving style vehicle brake cylinder pressure changes.

Table 2 shows the simulated fuel consumption for different driving styles under 0% and 5% slope conditions. From the table, it can be seen that there was a significant difference in fuel consumption under different slope conditions, but the difference in fuel consumption was relatively small under different driving styles. This is because the control method used in this article has a high accuracy in identifying driving style and controlling speed, allowing the required speed to be achieved at a low throttle opening. Therefore, the cumulative fuel consumption standard deviation is 0.010, which is less than 0.089 on a 5% slope, and the difference is not significant. In addition, the control method used in this article incorporates the rate of change in acceleration and speed indicators in the fuzzy inference of control weights to measure the changes in driving behavior and environment between the current driving state and the next moment. Its control weights are also related to real-time change indicators, resulting in small differences in fuel consumption between different driving styles. At the same time, it also indicates that the control method proposed in this article has universality, causing the fuel consumption under the different driving styles to tend to be similar to ecological driving.

**Table 2.** Fuel consumption for different slopes and driving styles.

| Slope (%) | | 0 | | | 5 | |
|---|---|---|---|---|---|---|
| Driving style | Calm | Moderate | Aggressive | Calm | Moderate | Aggressive |
| Fuel consumption (g) | 54.83505 | 54.81837 | 54.84242 | 69.29926 | 69.09475 | 69.13313 |

## 4. On-Road Test Results

To verify the effectiveness of the control strategy proposed in this article, vehicles located in an actual driving dataset of a continuous 9000 m on National Highway 236 were selected as the basis for simulation, as Figure 18 shows. The labels for the driving styles of the vehicles on this section were acquired by classifying the driving styles in the preceding section, and the simulation platform incorporated the actual speed and road conditions. The approach put forth in this paper (DS-MPC) should be contrasted with that of PID control in a system for fixed speed cruise control.

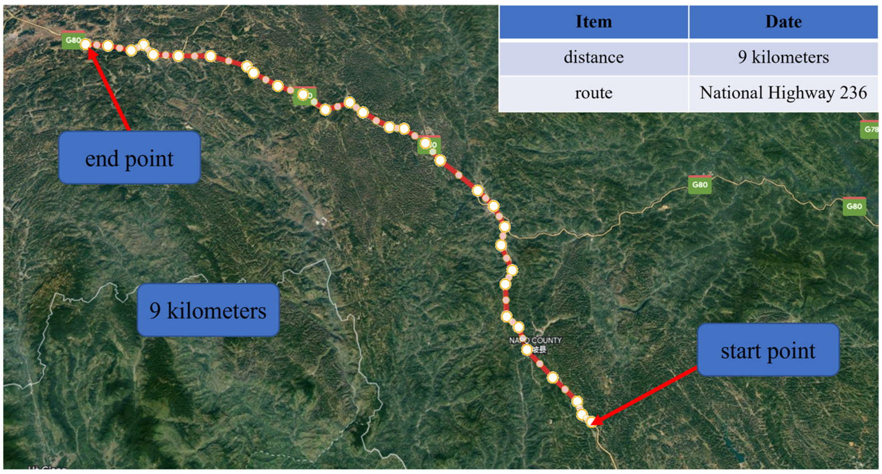


**Figure 18.** National Highway 236 test route.

Figures 19 and 20 display the speed tracking and corresponding error curves under real operating conditions. The results indicate that the control method proposed in this paper effectively tracks the speed changes of heavy trucks, maintaining a low deviation in speed. The average error is 0.03147 m/s, indicating an improvement of 80.56% over the accuracy of PID control. Furthermore, the standard deviation is 0.03210 m/s, indicating an improvement of 65.81% over the speed maintenance performance of PID control. Consequently, the proposed control method significantly enhances the power performance and road safety of the intelligent driving assistance system for heavy-duty trucks.

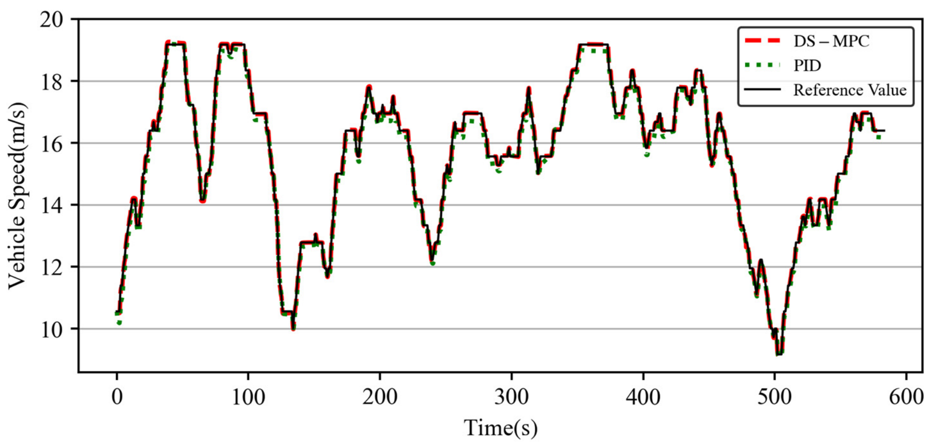


**Figure 19.** DS-MPC and PID speed tracking curve under actual working conditions.

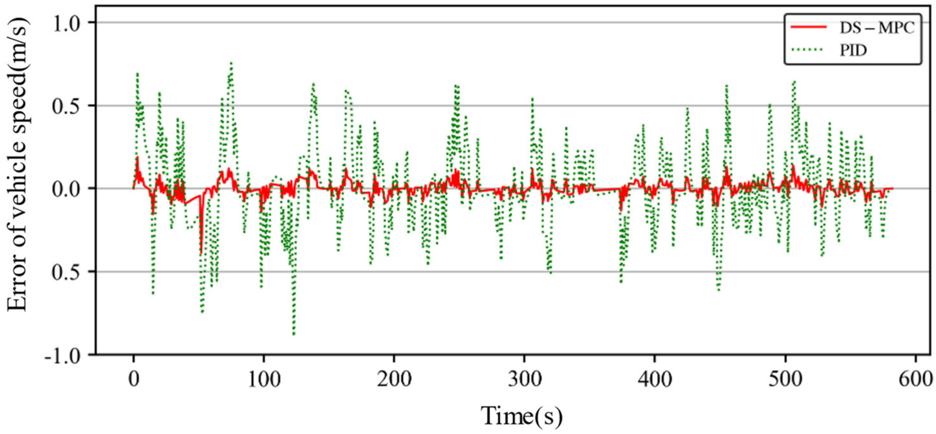


**Figure 20.** DS-MPC and PID speed tracking error curve under actual working conditions.

Figure 21 shows the fuel consumption comparison results of vehicles using DS-MPC control and PID control on this road section. As shown in the figure, during continuous changes in road slope, the total fuel consumption of vehicles using DS-MPC control method was 319.111g, while the fuel consumption of vehicles using the traditional control method was 329.881, with an average fuel saving rate of 3.27%, which constitutes a good fuel saving effect. In addition, the fuel consumption using the DS-MPC control method varied slightly under different driving styles, which is consistent with the fuel consumption results of the simulation results. But the fuel saving effects varied under different driving styles, with aggressive driving styles having a more significant reduction in fuel consumption. This is because after the DS-MPC control method accurately identifies the driving style, the changes in throttle opening and brake pressure of the aggressive driving style are smoother than those of the PID control method, thus achieving higher fuel efficiency. In summary, heavy-duty vehicles using the DS-MPC control method have high fuel efficiency and will effectively reduce emissions.

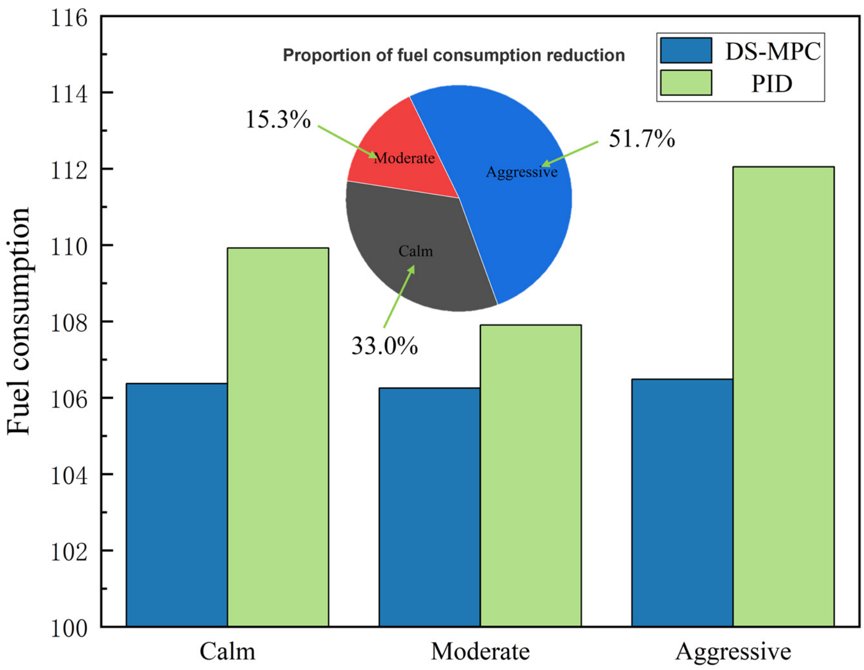


**Figure 21.** DS-MPC and PID fuel consumption under actual working conditions.

The elevation changes of the vehicle under actual operating conditions are depicted in Figure 22. To further illustrate the correlation between elevation changes and vehicle speed, Figure 23 presents typical slope sections along with their corresponding changes in vehicle speed. The proposed method outlined in this paper exhibits superior speed tracking performance on typical slope sections within the same road section. DS-MPC can enhance the precision of speed tracking during the deceleration process, thereby ensuring a uniform speed change. During the deceleration process, the vehicle has the ability to reach its predetermined target ahead of schedule and then enhance its acceleration. In comparison to PID control, it can achieve the desired vehicle speed in a shorter time. Furthermore, the DS-MPC algorithm is capable of effectively tracking the target speed during the deceleration phase, with a minimal overshoot and error, thereby achieving rapid tracking. It maintains good stability during the phase of increasing speed and further enhances the safety of road driving.

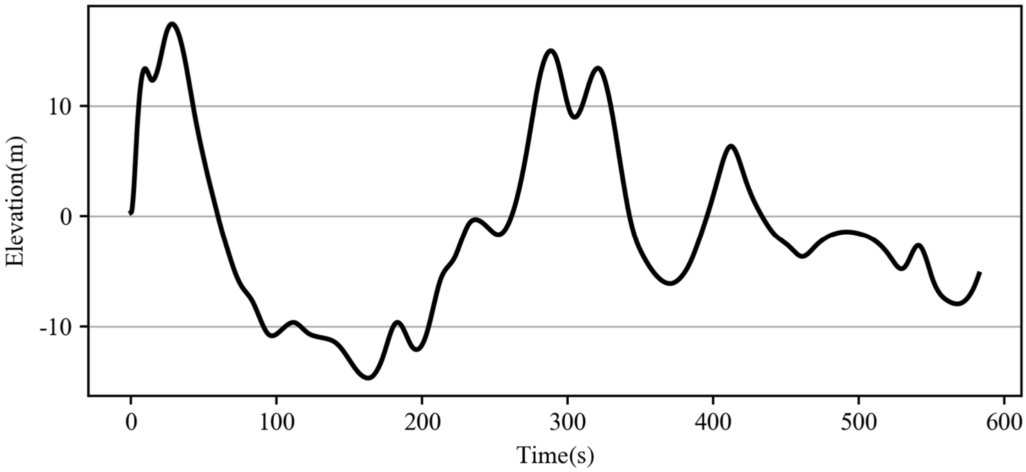


**Figure 22.** Vehicle elevation changes under actual working conditions.

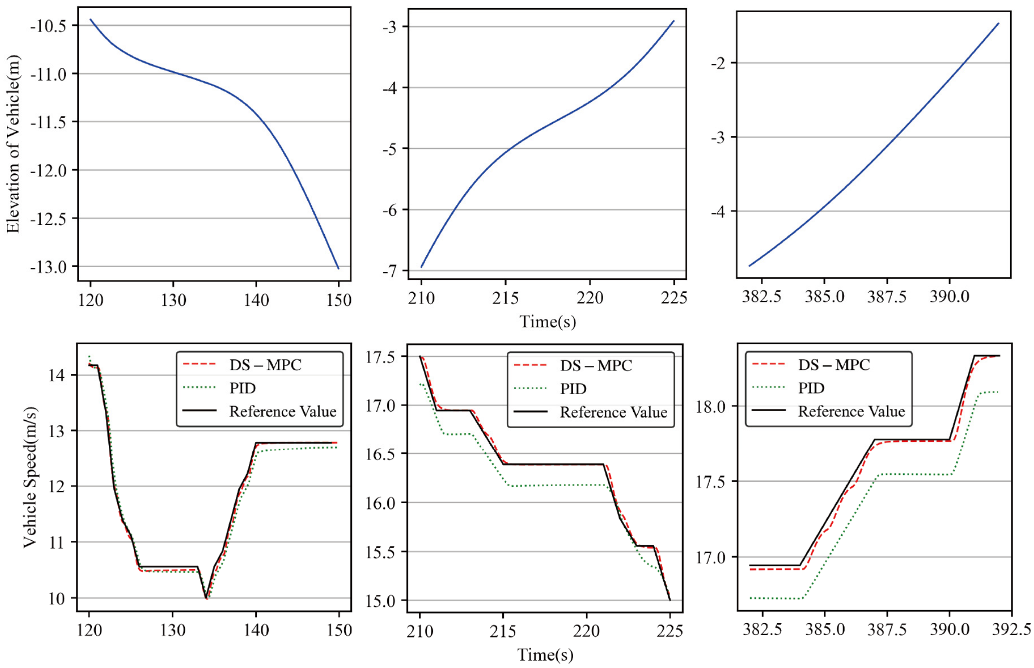


**Figure 23.** Typical slope section speed tracking under actual working conditions.

## 5. Conclusions and Prospects

Changes in driving style and the road environment are significant factors that influence eco-driving. This study newly integrates the elements of driving style and road gradient changes into the vehicle longitudinal control model, enabling the control system to adaptively recognize various driving styles and road conditions for improved control outcomes. Compared to traditional cruise control systems, the accuracies of speed control and fuel consumption have been enhanced. The development of an eco-driving oriented vehicle longitudinal control model can reduce development costs and enhance development efficiency simultaneously. This approach serves as a practical method to achieve energy-saving driving and enhance road safety. The conclusions are as follows:

(1) The proposed spectral clustering driving style recognition method based on a Bi-LSTM autoencoder successfully distinguishes different types of driving styles under ecological driving behavior.
(2) A fuzzy inference logic was devised to adaptively modify the control weights of the objective function taking into account factors such as driving style, slope, acceleration change rate, and vehicle speed.
(3) The proposed DS-MPC control method is more accurate and economical than traditional control methods under real working conditions.
(4) The proposed DS-MPC control method is highly versatile and yields significant and consistent optimization effects on fuel consumption, regardless of the slope and driving style, resulting in a fuel savings of 3% to 4% on average.

This research is a study aimed to improve the speed control accuracy of heavy-duty truck driving assistance systems and simultaneously reduce fuel consumption. However, the DS-MPC control method proposed in this paper does not categorize and identify the driving styles of heavy vehicles under different road conditions (e.g., urban and rural areas). Therefore, there is a need to identify driving styles under different road conditions by exploring more accurate methods to initialize the raw labels of the data in future research. In addition, the control strategy proposed in this paper can be deeply optimized to improve control accuracy by combining asymptotic tracking and neural adaptive learning algorithms with anti-perturbation.

**Author Contributions:** Conceptualization, Y.Z. and H.C.; methodology, W.G.; software, Y.Z. and H.C.; validation, L.Y., X.C. and M.P.; formal analysis, X.C.; investigation, L.Y.; resources, X.C.; data curation, L.Y.; writing—original draft preparation, Y.Z.; writing—review and editing, L.Y. and W.G.; visualization, L.Y.; supervision, M.P.; project administration, W.G.; funding acquisition, M.P. All authors have read and agreed to the published version of the manuscript.

**Funding:** This research was funded by [Guangxi University Sugarcane Research Fund] grant number [2022GZB008] and the National Natural Science Foundation of China [U23A202599].

**Institutional Review Board Statement:** Not applicable.

**Informed Consent Statement:** Not applicable.

**Data Availability Statement:** The datasets generated during and/or analyzed during the current study are available from the corresponding author on reasonable request.

**Conflicts of Interest:** The authors declare no conflict of interest.

## Abbreviations

| | |
|---|---|
| Bi-LSTM | Bidirectional long-short term memory |
| DS-MPC | Driving style-model predictive control |
| NEDC | New European driving cycle |
| WOA | The whale optimization algorithm |
| ADAS | Advanced driver assistance system |
| K-means | k-means clustering algorithm |

## References


1. Alam, M.S.; McNabola, A. A critical review and assessment of Eco-Driving policy & technology: Benefits & limitations. *Transp. Policy* **2014**, *35*, 42–49.
2. Chen, B.; Xu, C.; Wu, Y.; Li, Z.; Song, M.; Shen, Z. Spatiotemporal carbon emissions across the spectrum of Chinese cities: Insights from socioeconomic characteristics and ecological capacity. *J. Environ. Manag.* **2022**, *306*, 114510. [CrossRef] [PubMed]
3. Safari, G.H.; Asl Hashemi, A.; Yaghoobi Roodposhti, F. Eco-driving technology: An effective and economical approach to reduce fuel consumption and greenhouse gas. *J. Environ. Sci. Stud.* **2023**, *8*, 5960–5976.
4. Berkowicz, R.; Winther, M.; Ketzel, M. Traffic pollution modelling and emission data. *Environ. Model. Softw.* **2006**, *21*, 454–460. [CrossRef]
5. Du, W.; Chen, L.; Wang, H.; Shan, Z.; Zhou, Z.; Li, W.; Wang, Y. Deciphering urban traffic impacts on air quality by deep learning and emission inventory. *J. Environ. Sci.* **2023**, *124*, 745–757. [CrossRef]
6. Huang, Y.; Ng, E.C.; Zhou, J.L.; Surawski, N.C.; Chan, E.F.; Hong, G. Eco-driving technology for sustainable road transport: A review. *Renew. Sustain. Energy Rev.* **2018**, *93*, 596–609. [CrossRef]
7. Yu, S.; Pan, X.; Georgiou, A.; Chen, B.; Jaimoukha, I.M.; Evangelou, S.A. A Robust Model Predictive Control Framework for Ecological Adaptive Cruise Control Strategy of Electric Vehicles. In Proceedings of the 2023 IEEE International Conference on Mechatronics (ICM), Loughborough, UK, 15–17 March 2023; pp. 1–6.
8. Lu, X.Y.; Hedrick, J.K. Heavy-duty vehicle modelling and longitudinal control. *Veh. Syst. Dyn.* **2005**, *43*, 653–669. [CrossRef]
9. Wu, W.; Chu, X.; Liu, C.; Zheng, H.; He, Z. Predictive longitudinal following control for ship platoon considering diesel engine driven propeller reversal. *Ocean. Eng.* **2022**, *263*, 112231. [CrossRef]
10. Simorgh, A.; Marashian, A.; Razminia, A. Adaptive pid control design for longitudinal velocity control of autonomous vehicles. In Proceedings of the 2019 6th International Conference on Control, Instrumentation and Automation (ICCIA), Sanandaj, Iran, 30–31 October 2019; pp. 1–6.
11. Azızıaghdam, E.T.; Alankuş, O.B. Longitudinal control of autonomous vehicles consisting power-train with non-linear characteristics. *IEEE Trans. Intell. Veh.* **2021**, *7*, 133–142. [CrossRef]
12. Ji, W.; Lu, Z.; Tian, G. An Adaptive MPC Slip Controller for Hub Motor Driven Vehicles with a Novel Linearization Method. In Proceedings of the 2022 International Symposium on Electrical, Electronics and Information Engineering (ISEEIE), Chiang Mai, Thailand, 25–27 February 2022; pp. 272–277.
13. Yang, G. Asymptotic tracking with novel integral robust schemes for mismatched uncertain nonlinear systems. *Int. J. Robust Nonlinear Control.* **2023**, *33*, 1988–2002. [CrossRef]
14. Yang, G.; Yao, J.; Dong, Z. Neuroadaptive learning algorithm for constrained nonlinear systems with disturbance rejection. *Int. J. Robust Nonlinear Control.* **2022**, *32*, 6127–6147. [CrossRef]
15. Lee, J.; Choi, S.B. Integrated Control of Steering and Braking for Path Tracking using Multi-Point Linearized MPC. *IEEE Trans. Intell. Veh.* **2022**, *8*, 3324–3335. [CrossRef]
16. Wang, Z.; Dridi, M.; El Moudni, A. Co-Optimization of Eco-Driving and Energy Management for Connected HEV/PHEVs near Signalized Intersections: A Review. *Appl. Sci.* **2023**, *13*, 5035. [CrossRef]
17. Wang, P.; Ye, R.; Zhang, J.; Wang, T. An eco-driving controller based on intelligent connected vehicles for sustainable transportation. *Appl. Sci.* **2022**, *12*, 4533. [CrossRef]
18. Fafoutellis, P.; Mantouka, E.G.; Vlahogianni, E.I. Eco-driving and its impacts on fuel efficiency: An overview of technologies and data-driven methods. *Sustainability* **2020**, *13*, 226. [CrossRef]
19. Chu, H.; Li, Z.; Wang, J.; Hong, J. Fuel-Saving-Oriented Collaborative Driving Strategy for Commercial Vehicles Based on Driving Style Recognition. *Energies* **2023**, *16*, 6163. [CrossRef]
20. Pan, C.; Huang, A.; Chen, L.; Cai, Y.; Chen, L.; Liang, J.; Zhou, W. A review of the development trend of adaptive cruise control for ecological driving. *Proc. Inst. Mech. Eng. Part D J. Automob. Eng.* **2022**, *236*, 1931–1948. [CrossRef]
21. Jia, Y.; Nie, Z.; Wang, W.; Lian, Y.; Guerrero, J.M.; Outbib, R. Eco-driving policy for connected and automated fuel cell hybrid vehicles platoon in dynamic traffic scenarios. *Int. J. Hydrog. Energy* **2023**, *48*, 18816–18834. [CrossRef]
22. Peng, J.; Chen, W.; Fan, Y.; He, H.; Wei, Z.; Ma, C. Ecological Driving Framework of Hybrid Electric Vehicle Based on Heterogeneous Multi Agent Deep Reinforcement Learning. *IEEE Trans. Transp. Electrif.* **2023**. [CrossRef]
23. Deml, B.; Freyer, J.; Farber, B. Ein Beitrag zur Pradiktion des Fahrstils. *VDI Berichte* **2007**, *2015*, 47.
24. Biral, F.; Da Lio, M.; Bertolazzi, E. Combining safety margins and user preferences into a driving criterion for optimal control-based computation of reference maneuvers for an ADAS of the next generation. In Proceedings of the IEEE Proceedings. Intelligent Vehicles Symposium, Las Vegas, NV, USA, 6–8 June 2005; pp. 36–41.
25. Kalra, N.; Goyal, R.K.; Parashar, A.; Singh, J.; Singla, G. Driving Style Recognition System Using Smartphone Sensors Based on Fuzzy Logic. *Comput. Mater. Contin.* **2021**, *69*, 1968–1978. [CrossRef]
26. Almadi, A.I.; Al Mamlook, R.E.; Almarhabi, Y.; Ullah, I.; Jamal, A. A fuzzy-logic approach based on driver decision-making behavior modeling and simulation. *Sustainability* **2022**, *14*, 8874. [CrossRef]
27. Zdravković, S.; Vujanović, D.; Stokić, M.; Pamučar, D. Evaluation of professional driver's eco-driving skills based on type-2 fuzzy logic model. *Neural Comput. Appl.* **2021**, *33*, 11541–11554. [CrossRef]

28. Syed, F.U.; Filev, D.; Ying, H. Fuzzy rule-based driver advisory system for fuel economy improvement in a hybrid electric vehicle. In Proceedings of the NAFIPS 2007-2007 Annual Meeting of the North American Fuzzy Information Processing Society, San Diego, CA, USA, 24–27 June 2007; pp. 178–183.
29. Topić, J.; Škugor, B.; Deur, J. Synthesis and feature selection-supported validation of multidimensional driving cycles. *Sustainability* **2021**, *13*, 4704. [CrossRef]
30. Tao, J.; Zhang, R. Intelligent feature selection using GA and neural network optimization for real-time driving pattern recognition. *IEEE Trans. Intell. Transp. Syst.* **2021**, *23*, 12665–12674. [CrossRef]
31. Yang, Y.; Cao, T.; Xu, S.; Qian, Y.; Li, Z. Influence of driving style on traffic flow fuel consumption and emissions based on the field data. *Phys. A Stat. Mech. Its Appl.* **2022**, *599*, 127520. [CrossRef]
32. Sun, X.; Cai, Y.; Wang, S.; Xu, X.; Chen, L. Optimal control of intelligent vehicle longitudinal dynamics via hybrid model predictive control. *Robot. Auton. Syst.* **2019**, *112*, 190–200. [CrossRef]
33. Weißmann, A.; Görges, D.; Lin, X. Energy-optimal adaptive cruise control combining model predictive control and dynamic programming. *Control. Eng. Pract.* **2018**, *72*, 125–137. [CrossRef]
34. Zhai, C.; Luo, F.; Liu, Y.; Chen, Z. Ecological cooperative look-ahead control for automated vehicles travelling on freeways with varying slopes. *IEEE Trans. Veh. Technol.* **2018**, *68*, 1208–1221. [CrossRef]
35. Hussien, A.G.; Hassanien, A.E.; Houssein, E.H.; Bhattacharyya, S.; Amin, M. S-shaped binary whale optimization algorithm for feature selection. In *Recent Trends in Signal and Image Processing: ISSIP 2017*; Springer: Singapore, 2019; pp. 79–87.
36. Mafarja, M.; Qasem, A.; Heidari, A.A.; Aljarah, I.; Faris, H.; Mirjalili, S. Efficient hybrid nature-inspired binary optimizers for feature selection. *Cogn. Comput.* **2020**, *12*, 150–175. [CrossRef]
37. Von Luxburg, U. A tutorial on spectral clustering. *Stat. Comput.* **2007**, *17*, 395–416. [CrossRef]
38. Mondal, S.; Gupta, A. Assessment of vehicles headway during queue dissipation at signal-controlled intersection under mixed traffic. *Curr. Sci.* **2019**, *116*, 437–444. [CrossRef]